Modeling and Assessment of the Fault Ride-Through Capabilities of Grid Supporting Inverter-Based Microgrids

Elutunji Buraimoh
Department of Electrical Power Engineering
Durban University of Technology
Durban, South Africa
elutunji@gmail.com

Innocent E. Davidson
Department of Electrical Power Engineering
Durban University of Technology
Durban, South Africa
InnocentD@dut.ac.za

***Abstract*—Grid-connected micro-grids are subject to grid disturbances. This has undesirable effects on system operation. Riding through fault conditions is a crucial technical challenge. Evolving grid codes require micro-grids to possess fault ride-through capabilities and support the grid voltage recovery to imitate the behavior of the traditional electrical power systems. The paper proposes two models of a grid supporting inverter-based microgrid; the first controlled as a current source with a parallel impedance suitable for grid feeding applications; the second regulated as a voltage source with a virtual impedance suitable for grid forming applications. The main objective of these two systems is to achieve controlled power delivery to the grid using grid voltage and frequency regulation. This paper discusses power interaction under steady states and transient conditions. Grid voltage parameters, such as amplitude, phase angle, and frequency, are estimated using a synchronization system, as these are necessary for precise active and reactive power control. Results obtained provide an understanding of grid fault impact on grid supporting systems and fault ride-through compliance and evaluates the impacts of the virtual impedances on fault ride through and power interaction.**

***Index Terms*—microgrid, inverter, microgrid control, modeling, virtual impedance.**

I. Introduction

Distributed Generators (DGs) are core elements of the Renewable Energy Sources (RES) integration in grids and microgrids. The utility grid senses microgrid as a single component operating under suitable control schemes with a cluster of loads and DG units operated in coordination to reliably supply electricity connected to the host grid at the point of common coupling (PCC) [1]. Microgrid serves as a proper platform for optimal utilization of RES by providing advanced levels of operation and control. These control and operational features make microgrids capable of playing a critical role in ensuring and enhancing the stability of the future electrical network with increased integration of RES.

Thus, grid codes regulating DG connection to the grid need continuous amending. Microgrids experience several grid disturbances with the potentials of unwanted consequences on microgrid sources operation and local loads. Riding through such anomalous circumstances is a crucial technical challenge in microgrids [2]. In the past, grid code standards stipulate DG disconnection in the case of grid faults and disturbances [3], but this is no longer the case in amended grid codes. Nevertheless, with increasing renewable energy penetration in the medium and high voltage networks, sudden disconnection such sources impedes overall system reliability and stability [4][5].

In the wind energy system, for example, the fault ride-through (FRT) conditions require wind farms to remain grid-connected and provide ancillary services to the grid during grid fault [6]. Similarly, FRT capabilities are required of IPP based solar PV farms connected to the grid. Consequently, amended grid codes are with stipulations that require microgrids to possess FRT capabilities and support the grid voltage recovery to imitate the behavior of the traditional power systems. Consequently, DGs are expected to weather dip in grid voltage under a specified time [7]. Generally, microgrids possess the ability to operate in grid-synchronous and islanded modes and the additional capability of switching between these modes [3]. The main grid supplies the power deficit. The host grid under grid-synchronous operation absorbs excess power generated. However, the aggregate power generated within microgrids is expected to balance the local load demand at any point in time [1].

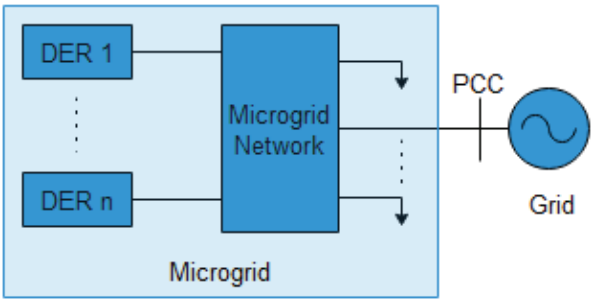

Figure 1. Schematic of a multiple-DER microgrid.

DG integration through MGs introduces operational challenges that should be addressed in the control design in order to ensure significant uncompromised reliability and optimally harnessing DG potential. Under [1], challenges most relevant to microgrid protection and control include: modeling, low inertia, instability, and bidirectional power flows. In modeling, the predominance of balanced three-phase conditions, inductive lines, and constant loads are valid

978-1-7281-9384-7/20/$31.00 ©2020 IEEE

concepts in traditional power systems modeling. However, these are not necessarily valid for microgrids, and consequently, models need to be revised [1].

The control scheme of a given microgrid system is required to overcome the listed challenges and guarantee reliability and cost-effectiveness. For instance, a control scheme must ensure that DER output voltages and currents track their references and ensure the damping of oscillations. Furthermore, a control scheme must ensure power balance and sudden load changes while keeping voltage and frequency deviations within acceptable limits.

The virtual impedance concept is a reality with an adjustable virtual output impedance used for power-sharing control between parallel inverters and limiting over-currents under grid faults. This impedance adjusts the reference of the inverter output voltage. Its value regulates the controller's dynamics. Thus, it is a variable in the control scheme and specified according to the inverter rated power. In this study, models of grid supporting inverter-based microgrid systems with similar parameters were developed. The first grid-supporting grid-feeding (gsg-feeding) system and the second grid-supporting grid-forming (gsg-forming) system with a virtual impedance for its unique operation. The main objective of these two systems is to participate in grid frequency and voltage regulation by active and reactive power control. The paper provides an overview of the power interaction between the supporting systems and the grid subjected to disturbances. A synchronization system was used to estimate the grid voltage parameters; amplitude, phase angle, and frequency, as these are necessary for precise active and reactive power regulation. Simulation results provide model insight and understanding of the grid fault impact on the two systems with a view of assessing the compliance of the modeled systems with the grid code requirements for fault ride-through. In addition, the impacts of the virtual impedances on FRT and power interaction were evaluated on the gsg-forming.

II. Inverter-Based Microgrids Control Strategies

The controls of an inverter-based microgrid are classified as grid feeding, grid supporting, and grid forming depending on the operation mode. The grid-forming inverter-based microgrid is represented as an ideal ac voltage source with a low output impedance with the ability to fix local grid frequency and voltage magnitude.

However, the grid-feeding system is required for power injection into an already constrained powered grid. This grid feeding is denoted by a grid-connected ideal current source in parallel with large impedance. Furthermore, grid-supporting inverter-based microgrids regulate their output current and voltage to keep the grid frequency and voltage amplitude close to their nominal values. Grid-supporting systems as earlier stated, could be the current source (gsg-feeding) or voltage source (gsg-forming). In gsg-forming, the link impedance influence is usually mimicked by internal control.

A gsg-feeding requires at least a grid former to form a grid and stipulate voltage reference for its operation. Consequently, this system is not deployed for island operations independently. However, a gsg-forming system mainly operates in island mode because it can inherently stipulate grid voltage. The grid-supporting systems are in between grid-feeding and grid-forming systems, with the distinctive task of controlled active and reactive power injection to regulate grid frequency and voltage respectively.

Lastly, the control of a g-supporting system as a voltage source with link impedance enables both standalone and grid-synchronous operation mode[6][8]. This is similar to the typical operation of a synchronous generator in a conventional grid.

TABLE I. Summary of Inverter-Based Microgrid Controls

Inverter type	Source type	Control type	Operation modes
Grid feeding	Ideal current source	Sets P and Q references	Grid-connected
Grid forming	Ideal voltage source	Sets V and f references	Islanded
Grid-supporting (current source)	Droop controlled current source	P and Q control using f and V references	Both grid-connected and islanded
Grid-supporting (voltage source	Droop controlled voltage source	V and f control using Q and P references	Both grid-connected and islanded

III. Modeling and Control Grid Supporting Systems

A flexible microgrid must possess the ability to control active and reactive power flows, import and export power to and fro main grid, and efficiently handle the energy storage systems. The power electronic interfaces are deployed between DER and the rest of the grid to actualize this level of flexibility [9][10][11]. The simple microgrid schematics in Fig. 2 show a DER at bus 's' connected to a load at bus 'r' through line impedance Z=R+jX.

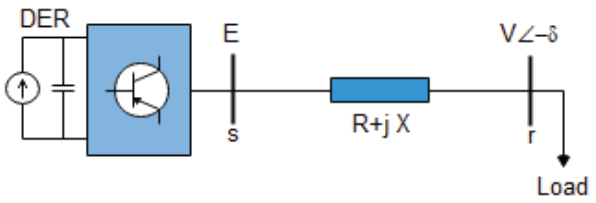

Figure 2. Inverter interfaced DER microgrid

The active power and reactive power delivered to the bus 's' is given by;

$$P = \frac{E^2}{Z}\cos\sigma - \frac{EV}{Z}\cos(\sigma+\delta)$$
$$Q = \frac{E^2}{Z}\sin\sigma - \frac{EV}{Z}\sin(\sigma+\delta) \quad (1)$$

The line impedance is Z, where σ is the impedance angle. Hence, the expression is re-expressed as follows;

$$P = \frac{E}{R^2 + X^2}\left[R\left(E - V\cos\delta\right) + XV\sin\delta\right]$$
$$Q = \frac{E}{R^2 + X^2}\left[-RV\sin\delta + X\left(E - V\cos\delta\right)\right] \quad (2)$$

Equations 1 and 2 confirms dependence output voltage V and its power angle δ on active power P and reactive power Q. Consequently, in an inductive line where X >> R;

$$\delta = \frac{PX}{EV} \quad (3)$$

$$E - V = \frac{XQ}{E} \quad (4)$$

Hence, in the inductive system, active power is controlled through frequency regulation, and voltage is controlled by reactive power.

Under this system specifically, DER output reactive power independently regulates inverter voltage, and DER active power independently regulate the frequency. Hence, Reactive Power-Voltage and Active Power-Frequency controls constitute droop control expressed by employing a linear approximation:

$$\omega^{**} = \omega^{*} - k_p\left(P^{*} - P_m\right)$$
$$E^{**} = E^{*} - k_q\left(Q^{*} - Q_m\right) \quad (5)$$

where E^* and ω^* are specified nominal voltage and frequency of an inverter-based microgrid. The *kp* and *kq* are droop coefficients of DER active power and reactive power. As expressed in equation 5, any change in frequency and voltage has impacts on the output active and reactive powers respectively. The droop characteristics define appropriate frequency and voltage deviations for the control [12]. The primary controls in Figs. 3 and 4 ensure prompt control in keeping power balance between generation and load demand at any point in time [10]. The voltage and frequency in a microgrid are always kept within the acceptable operational limit irrespective of the changes in the voltage and frequency and voltage indexes of a pulse width modulation (PWM) generator. Therefore, in grid-supporting systems, implemented droop techniques regulate the active and reactive power exchange with the grid to maintain the grid voltage and frequency. The droop concept imitates the dynamic characteristics of typical synchronous connected to the grid such that generated active power is decreased when the frequency rises and injected reactive power decreased under rising grid voltage amplitude. Under the instantaneous reactive power theory, the active power P_m and reactive power Q_m are estimated using:

$$P_m = \frac{3}{2}\left(v_d i_d + v_q i_q\right)$$
$$Q_m = \frac{3}{2}\left(v_d i_q - v_q i_d\right) \quad (6)$$

where v_d and v_q are the *d-q* components of the AC grid voltage while i_d and i_q are *d-q* components of the current.

A. Grid-Supporting Grid Feeding Mode

A grid-supporting inverter-based microgrid controlled as a current source is shown in Fig. 3.

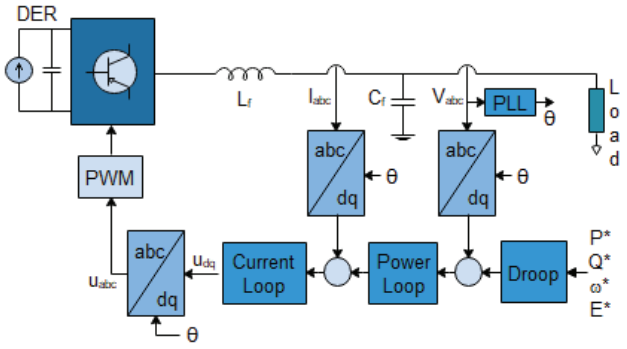

Figure 3. Grid-Supporting Grid Feeding control

The active power, reactive power, grid voltage, and frequency constitute major parameters for microgrid control. The frequency and PCC voltage are dominantly determined by the host grid when operated in the gsg-feeding mode. In this grid synchronous mode, the fundamental responsibility of microgrid control is to adjust the active power generated and reactive power injection by the DER. More importantly, injected reactive power is utilized in power factor correction, grid voltage support. The droop is introduced to allow the inverter to contribute to grid voltage magnitude and frequency regulation by adjusting the power (P and Q) delivery. The power control loop in Fig. 3 computes the current references, i^*_d, and i^*_q, using voltage direct-axes components v_d and the output of the droop power-sharing P^{**} and Q^{**} such that

$$i_d^* = \frac{2}{3}\frac{P^{**}}{v_d}$$
$$i_q^* = -\frac{2}{3}\frac{Q^{**}}{v_d} \quad (7)$$

B. Grid-Supporting Grid forming Mode

The gsg-forming system is considerably more challenging compared to gsg-feeding because it involves the implementation of precise load-sharing techniques to balance sudden active power mismatches. Microgrid frequency and voltage are not specified and supported by the main utility grid but are expected to be taken care of by the DER(s). The local primary controller ensures power balance using local measurements and the secondary controller dictates precise

set points to primary controllers each DER. As stated earlier, the system is controlled as a voltage source, as shown in Fig. 4. The droop loop in Fig. 4 compares the P_m and Q_m estimated in equation 6 with the reference P* and Q*. The errors obtained are multiplied with the droop gains as shown in equation 5 and used to obtain the new references for voltage and the angular frequency. This enables the grid supporting systems to actively participate in grid frequency and voltage amplitude regulation by controlling the active and reactive power.

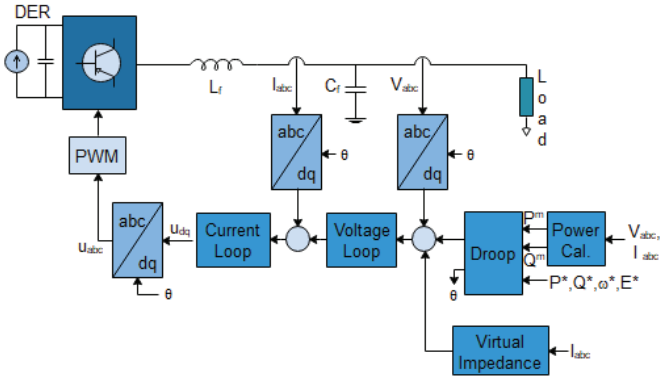

Figure 4. Grid-Supporting Grid Forming control

The inverter emulates a voltage source, as shown in Fig. 4 and connected to the rest of the grid using a link impedance similar to a typical synchronous generator. The active power generated and reactive power injected are functions of the grid voltage, inverter terminal voltage, and the link impedance. In this work, link impedance is not a physical impedance installed between the grid and the inverter, but a virtual component, imitated in the inner control loop. This inverter-based microgrid requires no grid-forming inverter when operated both in standalone and grid-connected modes. The simultaneous implementation of virtual impedance and droop controllers dynamically vary the microgrid operating parameters to fit instantaneous conditions. The outer voltage controller can also be realized with a PI control scheme such that the controller output is given by equation 8

$$i_d^* = \left(k_{pv} + \frac{k_{iv}}{s}\right)\left[v_d^* - v_d - v_{dpd}\right] \qquad (8)$$
$$i_q^* = \left(k_{pv} + \frac{k_{iv}}{s}\right)\left[v_d^* - v_q - v_{dpq}\right]$$

where k_{IV} and k_{PV} are the integral gain and proportional gain of the voltage PI control, respectively. The v_{dp} is the drop in voltage due to the grid or virtual impedance.

Furthermore, according to the current references, i^*_d and i^*_q, generated by the power control loop and voltage control loop in the two systems, the current control loop generates reference voltage (u_d and u_q) of direct-quadrature-axes for the PWM. This control is realized using a PI controller such that the controller output is expressed as

$$u_d = \left(k_{pi} + \frac{k_{ii}}{s}\right)\left[i_d^* - i_d\right] + v_d + (\omega L) \times i_q^* \qquad (9)$$
$$u_q = \left(k_{pi} + \frac{k_{ii}}{s}\right)\left[i_q^* - i_q\right] + v_q - (\omega L) \times i_d^*$$

IV. Implementation of Virtual Impedance Control

As an insightful measure to solve these drawbacks of the conventional droop control as it strongly depends on the gridline impedance, a substantial inductor could be employed in linking inverter to the ac grid and thus having a highly inductive line impedance. However, this is approach is inefficient and costly. The inverter dc-link voltage is significantly boosted to compensate for the depth of voltage drop across these inductors, thereby diminishing general efficiency. Introducing impedance virtually into the control instead of a physical link impedance is a more efficient and effective solution that is adapted in the control loop of an inverter-based microgrid. Consequently, the voltage drops in equation 8 over an inductive-resistive line is expressed as;

$$v_{dpd} = Ri_d - \omega L i_q + L\frac{di_d}{dt} \qquad (10)$$
$$v_{dpq} = Ri_q - \omega L i_d + L\frac{di_q}{dt}$$

Therefore, virtual impedance is implemented by subtracting equation 10 from the preferred voltage reference and measured voltage as shown in Fig 4.

$$v_{dpd} = Ri_d - \omega L i_q + \frac{\omega_c}{s+\omega_c} sLi_d \qquad (11)$$
$$v_{dpq} = Ri_q - \omega L i_d + \frac{\omega_c}{s+\omega_c} sLi_q$$

However, the high-frequency effects of the derivative terms are limited by introducing a low-pass filter (LPF) to the derivative terms, as expressed in equation 11 where ω_c is the cutoff frequency of the LPF. In Fig. 4, current limiting is not implemented in the current loop because this could cause voltage control loss and instability. Hence implementation is in the voltage loop and discussed in the results section.

V. Results and Discussion

The rate of change of the phase of a sinusoidal grid voltage waveform for the two grid supporting system models is shown in Fig. 5. These are used in estimating the phase angle in the systems. In the gsg-feeding system, the angular frequency of grid voltage estimated by the PLL and oscillated initially before a steady-state of synchronization is achieved with the grid voltage.

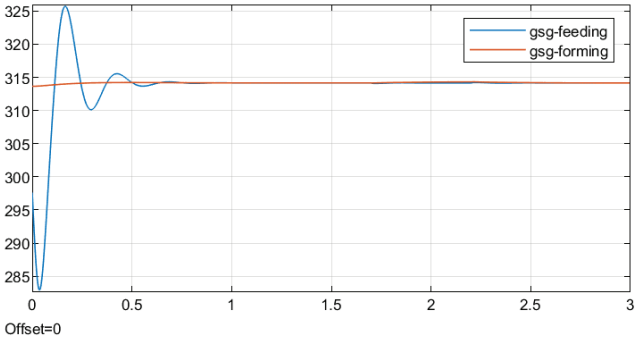

Figure 5. Angular frequencies of the Grid-Supporting systems

The estimated phase angles in both systems under the periods of grid synchronization and transient faults between time 1.7 and 2.2 seconds are shown in Fig 6.

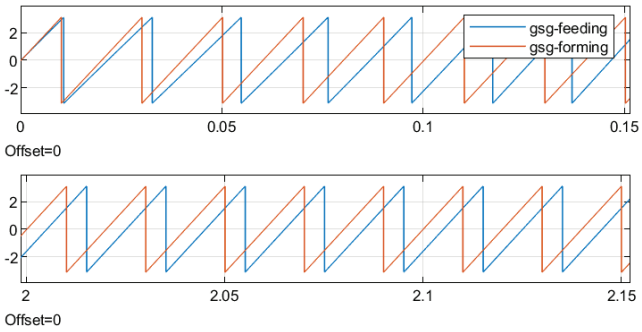

Figure 6. Phase angles of both systems

However, THD of the gsg-forming model output voltage waveform is significantly higher during start-up, under fault and seconds of post fault clearance, as shown in Fig. 7 reaching 36%, 8% and 7% in three instances.

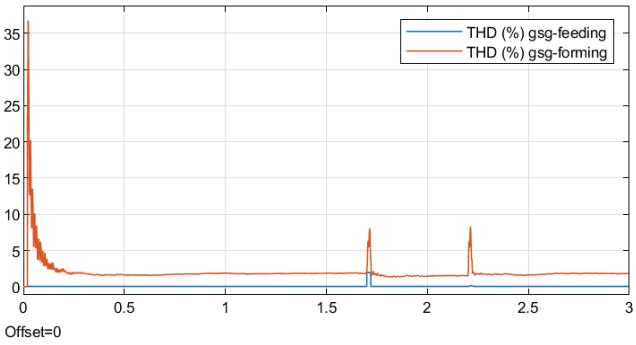

Figure 7. THD of output voltage waveforms

The frequency in a gsg-forming microgrid is slightly different from gsg-feeding microgrid, as revealed in the simulation results of Fig. 8. Under the gsg-forming system, the frequency changes rapidly in line with the droop control to attain stability. Although the microgrid is operated around the nominal frequency of 50 Hz. Under the synchronized operation with the main grid, the transients in frequency are not noticed.

It must be noted that frequency regulation and control is a challenging task in the gsg-forming system because inverter-based microgrids comprise of inertia-less DERs. However, some virtual inertia is provided by the power droop controllers. Prompt and precise estimation of parameters such as frequency and voltage are essential requirements for successful gsg-forming control and operation. Based on Fig. 8, gsg-forming microgrid must be equipped extensive energy storage system to accommodate rapid control. This will enable the system to meet up and adjust to the ever and fast-changing frequency and voltage within an allowed limit. Specific advanced methods are also available in case this rapid control of energy storage is insufficient to manage and restore voltage and frequency near the desired reference. Furthermore, droop control of DER units and controllable load could participate in voltage and frequency regulation under frequency and voltage droops.

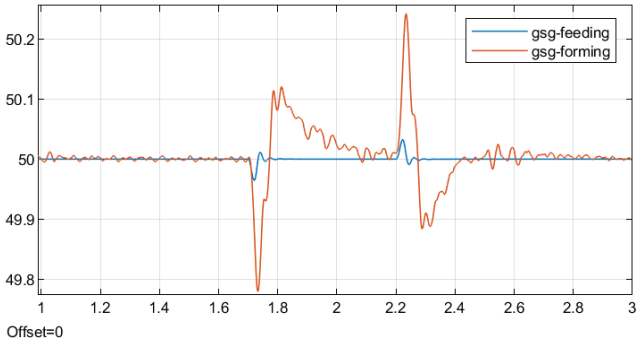

Figure 8. Frequencies under the grid supporting systems

Fig. 9 shows the RMS terminal voltage of inverter-based DERs of the microgrid in the grid supporting systems. Under the FRT requirements of the grid codes, the grid supporting systems withstood terminal voltage drop up to the specified percentage of nominal voltage at a given particular amount of time in seconds. However, in any case of a severe grid fault, the voltage could drop beyond the acceptance criteria of the grid code; thus, a secondary voltage control will be required. The corresponding output currents of the DERs in the two systems are given in Fig. 10

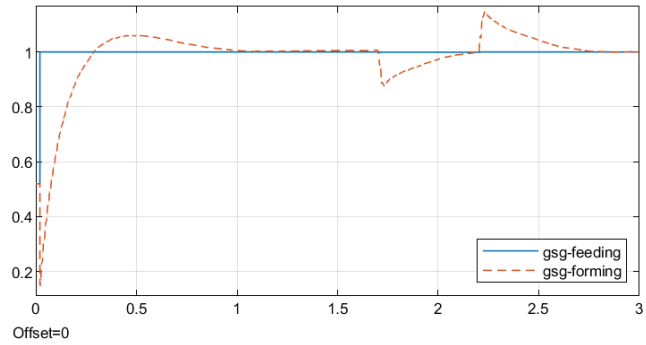

Figure 9. RMS voltages of the grid supporting systems

Fig. 11 shows the active power generation in the two systems. Power fluctuations are well suppressed in the grid-connected mode under the period of fault. However, the active power increased in the grid-supporting grid-forming due to the absence of any other swing system. This made the system contribute to the fault current, thereby increasing the grid current and, by extension, active power generation.

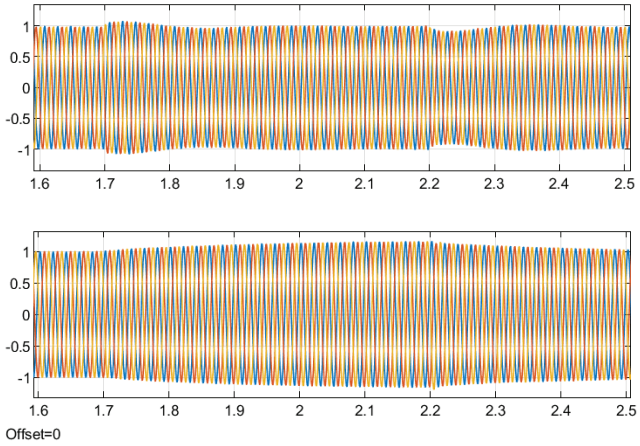

Figure 10. DER output current waveforms under fault

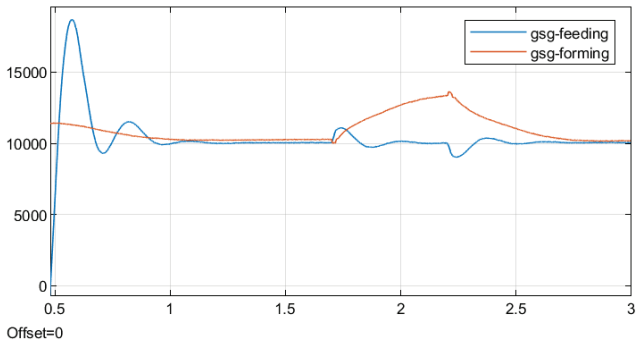

Figure 11. Active Power in the systems

Fig. 12 shows reactive power injection in the two systems. Consequently, the secondary control proposed earlier could provide reactive power support, especially during and after the clearance of fault especially in the grid supporting systems. This will coordinate active power injection under disturbances and ensure that active and reactive power generated fall within the apparent power rating of the inverter.

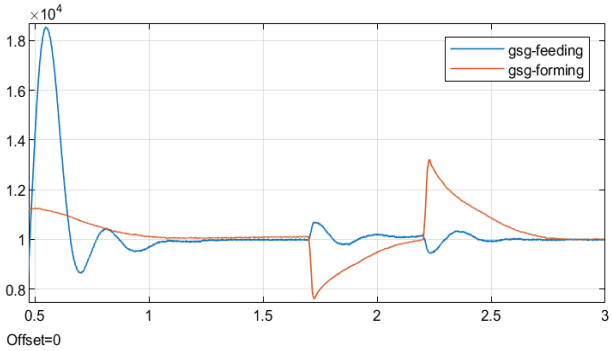

Figure 12. Reactive Power in the systems

Lastly, virtual impedances served as a fault current limiter in the gsg-forming system to limit the amplitude of the fault current under the grid fault. This, by extension, limited the active power generations under fault to reduce the fault current contribution as shown in Fig. 13. Furthermore, the virtual impedance makes the damped oscillations in the system. The fault current limitation provided by the virtual impedance is crucial to fulfilling the FRT requirement under faults and transient disturbances on the grid

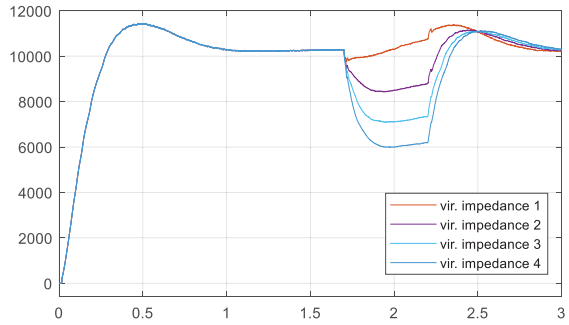

Figure 13. Gsg-Forming Active Power with increasing virtual impedance under fault

The effect of increasing virtual impedance is as shown in Fig 13 during a fault. Under fault, excessive current reference output of the voltage control loop is inhibited due to the presence of virtual impedance, which reduced voltage reference. Virtual impedance can be integrated with other distribution smart devices such as dynamic voltage restorer for the power quality enhancement and transient control in distribution systems. It must be noted that the value of the virtual line impedance should be more than the solid line impedance to have a significant influence on power and fault current limiting. Lastly, substantial virtual impedance also limits the output voltage and inhibits the amount of power delivered into the grid.

CONCLUSION

The grid supporting models of inverter-based microgrid has been developed with grid feeding and grid forming abilities using similar system parameters. Precise estimation of the grid parameters, voltage amplitude, phase angle, and frequency are necessary for an efficient control system. Based on the power interaction between the grid and the microgrid, the grid supporting the grid feeding model is suitable for the grid-connected mode of operation while and the grid supporting grid forming system with a virtual impedance is suitable for standalone operation. The droop controls used show good results for microgrid power-sharing.

Furthermore, virtual impedance mitigated some of the drawbacks in the grid supporting system when subjected to disturbances. The virtual impedance enhanced compliance with the grid code requirements for fault ride-through. The virtual impedance is implemented without undermining the system efficiency.

REFERENCES

[1] D. E. Olivares *et al.*, "Trends in microgrid control," *IEEE Transactions on Smart Grid*, vol. 5, no. 4, pp. 1905–1919, 2014.

[2] N. Jaalam, N. A. Rahim, A. H. A. Bakar, C. K. Tan, and A. M. A. Haidar, "A comprehensive review of synchronization methods for grid-connected converters of renewable energy source," *Renewable and Sustainable Energy Reviews*, vol. 59, pp. 1471–

1481, 2016.

[3] E. Buraimoh, I. E. Davidson, and F. Martinez-Rodrigo, "Fault Ride-Through Enhancement of Grid Supporting Inverter-Based Microgrid Using Delayed Signal Cancellation Algorithm Secondary Control," *Energies*, vol. 12, no. 20, p. 3994, Oct. 2019.

[4] L. Meegahapola, M. Datta, I. Nutkani, and J. Conroy, "Role of fault ride-through strategies for power grids with 100% power electronic-interfaced distributed renewable energy resources," *Wiley Interdisciplinary Reviews: Energy and Environment*, vol. 7, no. 4, p. e292, Jul. 2018.

[5] E. Buraimoh and I. E. Davidson, "Development of an IGBT-Diode based Fault Current Limiter for Fault Ride-Through Enhancement in Microgrid Application," in *IEEE PES/IAS PowerAfrica*, 2019, pp. 190–195.

[6] J. Rocabert, A. Luna, F. Blaabjerg, and P. Rodriguez, "Control of Power Converters in AC Microgrids," *IEEE Transactions on Power Electronics*, vol. 27, no. 11, pp. 4734–4749, 2012.

[7] A. M. Dissanayake and N. C. Ekneligoda, "Transient Optimization of Parallel Connected Inverters in Islanded AC Microgrids," *IEEE Transactions on Smart Grid*, vol. PP, no. c, pp. 1–12, 2018.

[8] A. Vinayagam, K. S. V. Swarna, S. Y. Khoo, A. T. Oo, and A. Stojcevski, "PV Based Microgrid with Grid-Support Grid-Forming Inverter Control-(Simulation and Analysis)," *Smart Grid and Renewable Energy*, vol. 08, no. 01, pp. 1–30, 2017.

[9] J. M. Guerrero, J. C. Vásquez, J. Matas, M. Castilla, and L. García de Vicuna, "Control strategy for flexible microgrid based on parallel line-interactive UPS systems," *IEEE Transactions on Industrial Electronics*, vol. 56, no. 3, pp. 726–736, 2009.

[10] H. Bevrani and S. Shokoohi, "An intelligent droop control for simultaneous voltage and frequency regulation in Islanded microgrids," *IEEE Transactions on Smart Grid*, vol. 4, no. 3, pp. 1505–1513, 2013.

[11] E. Buraimoh and I. E. Davidson, "Comparative Analysis of the Fault Ride-Through Capabilities of the VSG Methods of Microgrid Inverter Control under Faults," in *Proceedings - 2019 Southern African Universities Power Engineering Conference/Robotics and Mechatronics/Pattern Recognition Association of South Africa, SAUPEC/RobMech/PRASA 2019*, 2019.

[12] E. Buraimoh and I. E. Davidson, "Investigation of the Low Voltage Ride-Through of Inverter Using Virtual Inertia Methods in Microgrid," *International Journal of Engineering Research in Africa*, vol. 44, pp. 200–212, 2019.